Original Research Paper | Physics | Volume : 6 ¦ Issue : 2 ¦ Feb 2021 ¦ e-ISSN : 2456-5040

TO STUDY XRD ANALYSIS OF SAMARIUM IRON GARNET DUE TO AL DOPING

Shyamal Kumar Pal

Department of Physics, Bijoy Krishna Girl's College, Howrah, India

ABSTRACT

This study investigates the structural properties of Samarium Iron Garnet (SmIG) when doped with aluminium (Al). Samarium Iron Garnet, a material known for its unique magnetic and optical characteristics, exhibits changes in structural properties when doped with Al, a process that substitutes Fe ions with Al ions in the garnet lattice. By varying the concentration of Al, we aim to understand how this doping influences the crystal structure, lattice parameters, and microstructural features of SmIG. X-ray diffraction (XRD is employed to analyse the samples. The results indicate that Al doping leads to a slight contraction of the lattice parameters and alters the microstructure, suggesting changes in the crystallographic environment and bonding characteristics.

1. INTRODUCTION

The rare earth garnets have attracted the attention of the researchers due to their complex magnetic nature as well as their enormous potential of application in various fields from optical communication to magneto optical systems [1-3]. Several investigations have been conducted to study various magnetic parameters viz. magnetic susceptibility, magnetic anisotropy, temperature dependency of magnetization, exchange interactions etc. of these rare earth garnets [4-10]. The rare earth iron garnets are ferrimagnetic oxides with chemical formula $R_3Fe_5O_{12}$, where R stands for rare earth ions. According to Néel, the ferrimagnetic ordering in these materials arises due to the super exchange interactions among the magnetic sub lattices formed by the cations present in different voids. In these magnetic materials the Fe^{3+} ions present in the tetrahedral and octahedral voids are strongly coupled with each other whereas the rare earth ions in the dodecahedron voids are weakly coupled in an antiparallel direction. The resultant magnetic moment gives rise to the spontaneous magnetic ordering in the sample [4]. Among different garnets, Yttrium (Y), Samarium (Sm), Europium (Eu), Terbium (Tb) and Gadolinium (Gd) garnets have been found to be investigated widely by different researchers in last decades due to their poetical of applications [12–16]. Samarium iron garnet is one of the important members of this family.

In this present work the focused on the structural properties of samarium iron garnet and the effect of transitional metal ion doping in the lattice replacing the rare earth ions. The pure samarium iron garnet ($Sm_3Fe_5O_{12}$) and aluminium doped samarium iron garnet ($Sm_{2.7}Al_{0.3}Fe_5O_{12}$) prepared through sol-gel method by substituting the transition metal in place of the rare earth ion. Structure and surface morphology of both systems have been investigated using X-ray diffraction (XRD) and field emission scanning electron microscope (FESEM) data analysis.

2. EXPERIMENTAL

The first and the most essential requirement to work with a system after its preparation, is to determine its crystallographic phase. For this, the most efficient and convenient way is to analyse the X-ray diffraction (XRD) pattern of the prepared material. In addition to this, XRD pattern also provides information regarding lattice parameters, lattice strain, crystallite size, presence of other phases, etc.

2.1 Material and Methods

Nanocomposite of samarium iron garnet [SFG], and aluminium doped samarium iron garnet [ASFG] were prepared by wet chemical synthesis route using sol-gel chemical technique. To prepare samarium iron garnet nanoparticles, precursor materials of $Sm(NO_3)_3{\cdot}6H_2O$ (Sigma-Aldrich, 99.9% purity) and $Fe(NO_3)_3{\cdot}9H_2O$ (Merck, Germany) were taken. The precursor materials of $Sm(NO_3)_3{\cdot}6H_2O$, and $Fe(NO_3)_3{\cdot}\ 9H_2O$ were weighted keeping the stoichiometric ratio of samarium and iron as 3:5. For the preparation of SFG, the required precursor materials were taken in a beaker containing 100 ml deionized water. This mixture of salt and water then stirred for around one hour using Teflon coated magnetic beads and hot plate magnetic stirrer to prepare a complete homogeneous solution. The temperature of the hot plate was kept at ~40°C during the time of stirring. In the meantime, equimolar citric acid was taken in a beaker containing 200 ml of deionized water. To prepare a complete homogeneous citric acid solution this beaker was also kept over a magnetic stirrer containing the Teflon coated magnetic beads inside the solution and stirring was continued for around one hour. After the completion of one hour, the salt solution was started to stir vigorously at ~40°C and the homogeneous solution of citric acid was mixed drop wise in it. After completion of mixing the temperature of the final solution was increased to ~60°C and the stirring was further continued for another one hour to form a homogeneous solution of salt and citric acid. After this, the temperature of the solution was again increased to ~80°C and the stirring was continued for about 6 hours to obtain the sol. The heating and stirring of this sol were continued until a heavily dense form of the sol i.e. the gel was obtained. After obtaining the gel the stirring was discontinued and the temperature was increased to

~150°C. Due to this increased temperature the gel was found to get dried and an auto combustion reaction was initiated inside the gel. After completion of the auto combustion a highly porous material was obtained. Citric acid present here acts as a chelating agent by binding the metal cations as well as lowering the required temperature for reaction. This porous material was then crushed well in an agate mortar to obtain the as dried powder of the sample. The desired crystallographic phase of the sample was then obtained by sintering the as dried powder at a temperature of 900°C for 5 hours in a high precession muffle furnace where the rate of increase of temperature was 5°C per minute. This sintered material was again crushed well in an agate mortar to get the final powder sample. To prepare the aluminium doped samarium iron garnet (ASFG), same procedure as mentioned above was followed. In this case the precursor materials were $Sm(NO_3)_3 \cdot 6H_2O$ (Sigma-Aldrich, 99.9% purity), $Al(NO_3)_3 \cdot 9H_2O$ (Merck, Germany, purity 99% purity) and $Fe(NO_3)_3 \cdot 9H_2O$ (Merck, Germany). The precursor materials were weighted with stoichiometric ratio of samarium, aluminium and iron as 2.7:0.3:5.

The X-ray diffraction (XRD) patterns of the sample was recorded in powder X-ray diffractometer, model D8, BRUKER AXS, using Cu Kα radiation (λ = 1.5405 Å). For the confirmation of the crystallographic phase and to obtain the lattice parameters etc. this XRD data were analysed.

2.2 Results, Analysis and Discussions

XRD analysis

To know the crystallographic phase of the pristine and doped samples, XRD pattern of both the samples were recorded at RT using Copper K-α X-ray with average wavelength ~1.5406 Å in the 2θ range 10° to 80° and are shown in Fig. 4(i).

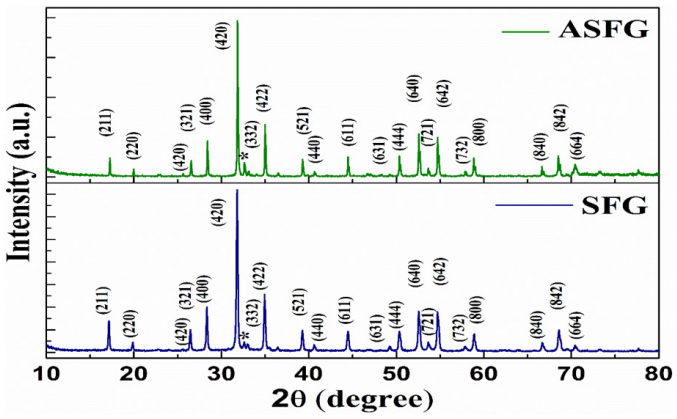

Figure 4(i): XRD patterns of the samples SFG and ASFG.

To confirm the phase purity of the samples, we tried to compare the peak positions obtained in XRD with the standard diffraction data base using JCPDS file no. 731379. From this study we observe that all the peaks and their relative intensities are consistent with the standard crystallographic database. From this we can confirm that both the pure and doped samples are of pure crystallographic phase. This also indicates that in case of ASFG the nanoparticles, aluminium has been successfully incorporated in the crystal replacing samarium in the garnet lattice. Thus, the prepared samples are of desired cubic crystallographic phase with space group $Ia\bar{3}d$. All the peaks are assigned with their corresponding crystallographic planes as per the JCPDS file and are shown in Fig. 4(ii). In both XRD data one peak with very small intensity has been found to appear which is shown by asterisk symbol in the figure. This peak belongs to $SmFeO_3$ crystallographic phase. The most intense peak (100%), with Miller indices (420) of the sample is observed at 2θ = 31.6°. Matching of all the peaks with the JCPDS file indicate formation of desired crystallographic phase which confirms that the Al^{3+} ions have successfully substituted the Sm^{3+} ions in the cubic crystal. To obtain the crystallite size of the sample the line broadening of the 100% intense peak of the XRD pattern is used in the well-known Scherrer equation (Eq. 3) as given in experimental section,

$$< D >= \frac{0.89\,\lambda}{\beta_{\frac{1}{2}} \cos\theta} \qquad (3)$$

Here, <D> is the average crystallite size, λ is the wavelength of the incident X-ray radiation, β1/2 is the full width at half maximum (FWHM) after subtracting the instrumental broadening and θ is the corresponding Bragg angle. The average crystallite size of the samples as estimated from the Scherrer equation are given as ~45 nm and ~42 nm for pure and doped sample respectively. This change in the crystallite size may be due to reduction in crystallite volume due to doping of smaller Al^{3+} ions in place of Sm^{3+} ions in the crystal lattice. The corresponding interplanar spacing (d) was calculated from the Bragg's equation (Eq. 1) as given in the experimental section;

$$2d\ sin\,\theta = n\lambda \qquad (1)$$

Here, '*n*' is the order of diffraction pattern. The lattice parameter '*a*' of the cubic garnet nanomaterials prepared was also calculated using the equation given as [29, 30];

$$\frac{1}{d^2} = \frac{h^2+k^2+l^2}{a^2} \qquad (4)$$

where, (*hkl*) are the Miller indices of the plane corresponding to the XRD peak. The corresponding values of and lattice parameter 'a' as obtained are ~12.6114 Å and ~12.5551 Å for SFG and ASFG respectively. This reduction in the value of lattice parameter in case of ASFG as compared to SFG may be due to the introduction of smaller Al^{3+} ions in place of Sm^{3+} ions in the garnet lattice. This explains the change in the crystallite size obtained from the XRD data discussed earlier.

3. CONCLUSION

Nanoparticles of $Sm_3Fe_5O_{12}$ and $Sm_{2.7}Al_{0.3}Fe_5O_{12}$ were successfully prepared using wet chemical method through sol-gel technique. The phase purity of the samples has been confirmed from the XRD data. Al^{3+} ions successfully replaced the Sm^{3+} ions of the crystal lattice.

4. REFERENCES

1. M. H. Phan,M. B.Morales, C.N. Chinnasamy, B. Latha,V. G. Harris, and H. Srikanth, Magnetocaloric effect in bulk and nanostructured Gd Fe O materials, J. Phys. D: Appl. Phys., vol. 42, p. 115007, 2009.
2. R. C. Booth and E. A.D.White, Magneto-optic properties of rare earth iron garnet crystals in the wavelength range 1.1–1.7 m and their use in device fabrication, J. Phys. D: Appl. Phys., vol. 17,

p. 579, 1984.
3. John S. McCloy and Brian Walsh, Sublattice Magnetic Relaxation in Rare Earth Iron Garnets, IEEE transactions on magnetics, VOL. 49, NO. 7, JULY 2013
4. Soshin Chikazumi, Physics of Ferromagnetism, Oxford University Press, 1997.
5. W.P. Wolf, R.M. Bozorth, Physical Review 124 (1961) 449.
6. K.P. Belov, S.A. Nikitin, Physica Status Solidi 12 (1965) 453.
7. G.P. Rodrigue, H. Meyer, R.V. Jones, Journal of Applied Physics 31 (1960) S376.
8. G.F. Dionne, Journal of Applied Physics 42 (1971) 2142.
9. K.P. Belov, M.A. Za˘ıtseva, A.V. Ped'ko, Soviet Physics JETP 36 (1959) 1191.
10. J.P. Hanton, IEEE Transactionson Magnetics 3 (1967) 505.
11. D.T.T. Nguyet, N.P. Duong, T. Satoh, L.N. Anh, T.D. Hien, Magnetization and coercivity of nanocrystalline gadolinium iron garnet, Journal of Magnetism and Magnetic Materials 332 (2013) 180–185.
12. H. Cao, H. Zheng, L. Fan, Z. Cheng, J. Zhou, Q. Wu, P. Zheng, L. Zheng, Y. Zhang, Structural, morphological, dielectric and magnetic properties of Zn-Zr co-doping yttrium iron garnet, Int J Appl Ceram Technol. 17 (2) (2020) 813–822.
13. U. Atzmony, E.R. Bauminger, A. Mustachi, I. Nowik, S. Ofer, M. Tassa, Anisotropy of the Europium-Iron Exchange Interaction in Rare-Earth Iron Garnets, Phys. Rev. 179 (1969) 514–522.
14. D.T.T. Nguyet, N.P. Duong, T. Satoh, L.N. Anh, T.T. Loan, T.D. Hien, Crystallization and magnetic characterizations of DyIG and HoIGnanopowders fabricated using citrate sol-gel, J. Sci.: Adv. Mater. Dev. 1 (2) (2016) 193–199.
15. S. Geller, J.P. Remeika, R.C. Sherwood, H.J. Williams, G.P. Espinosa, Magnetic Study of the Heavier Rare-Earth Iron Garnets, Phys. Rev. 137 (3A) (1965) A1034–A1038.
16. M. Adachi, H. Yamahara, M. Seki, H. Matsui and H. Tabata, Terahertz Magnonics Using Ultrathin Films of Samarium Ferrite Garnet, 2014 39th International Conference on Infrared, Millimeter, and Terahertz waves (IRMMW-THz), Tucson, AZ, (2014),1-2.
17. S.C. Parida, S.K. Rakshit, Z. Singh, Heat capacities, order–disorder transitions, and thermodynamic properties of rare-earth orthoferrites and rare-earth iron garnets, J. Solid State Chem. 181 (2008) 101–121.